Tunable Aharonov-Anandan phase in transport through mesoscopic hole rings

M. Pletyukhov* and U. Zülicke†

Institut für Theoretische Festkörperphysik and DFG Center for Functional Nanostructures, Universität Karlsruhe, D-76128 Karlsruhe, Germany

(Received 11 April 2008; published 7 May 2008)

We present a theoretical study of spin-3/2 hole transport through mesoscopic rings that is based on the spherical Luttinger model. A quasi-one-dimensional ring is created in a symmetric two-dimensional quantum well by a singular-oscillator potential for the radial in-plane coordinate. The quantum-interference contribution to the two-terminal ring conductance exhibits an energy-dependent Aharonov-Anandan phase, even though Rashba and Dresselhaus spin splittings are absent. Instead, confinement-induced heavy-hole–light-hole mixing is found to be the origin of this phase, which has ramifications for magnetotransport measurements in gated hole rings.

DOI: 10.1103/PhysRevB.77.193304 PACS number(s): 73.21.−b, 03.65.Vf, 73.23.Ad, 85.35.Ds

I. INTRODUCTION

Geometric quantum phases continue to be the subject of great interest because they rather elegantly elucidate quite complex fundamental microscopic properties.[1] The well-known Aharonov-Bohm[2] and Aharonov-Casher[3] effects are pertinent examples, as is the Berry phase[4] acquired by a quantum system during adiabatic cyclical variation of an external parameter. The more general concept of the Aharonov-Anandan (AA) phase[5] that arises in the cyclical evolution of a quantum state was later shown to subsume the above-mentioned three phenomena as special cases. The recent progress in our understanding of geometric phases was spurred by numerous experimental and theoretical studies.[6]

Modern nanofabrication techniques have made it possible to study quantum interference and, thus, geometric quantum phases in mesoscopic electronic devices.[7] The first theoretical suggestions[8] and experimental realizations[9] of electronic quantum interference devices were Aharonov-Bohm[2] interferometers. Subsequent theoretical studies predicted electronic signatures of Berry phases[10] and the Aharonov-Casher effect.[11–13] Inspired by possible applications in the burgeoning field of spintronics,[14] recent experimental efforts were devoted to observing tunable spin-related geometric phases in semiconductor rings subject to strong spin-orbit coupling.[15,16] In several of these experiments,[16] charge carriers moving through the ring structure are characterized by an intrinsic (spin) angular momentum equal to 3/2. This is due to the fact that the states in the uppermost valence band of typical semiconductors originate from p-like atomic orbitals of the material's constituent elements.[17] The same is true for the conduction-band states in HgCdTe quantum wells because of a band inversion. Here, we provide a careful study of the complexities that arise from the spin-3/2 character of the charge carriers confined in a mesoscopic ring. We identify a nontrivial part of the AA phase[5] that enters the interference contribution to the two-terminal ring conductance. The energy dependence of this geometric phase will result in a modulation of magnetoconductance (Aharonov-Bohm[2]) oscillations as a function of carrier density in the ring, e.g., when a gate voltage is applied. We trace the origin of the anomalous AA phase to a confinement-induced coupling between heavy-hole (HH) and light-hole (LH) states[18] that is ever present and unrelated to (Rashba or Dresselhaus) spin splitting due to (structural or bulk) inversion asymmetry.[17] Our analysis provides a framework for interpreting numerical results[19] and complements previous analytical calculations[13] wherein HH-LH mixing was neglected.

Below, we describe our theoretical model for hole rings. Readers who are not interested in mathematical details could skip to the end of this part, wherein results for the lowest ring subbands are presented. We then analyze the emerging energy-dependent AA phase and, in our concluding discussion, address implications for experiments.

II. THEORETICAL MODEL FOR A MESOSCOPIC HOLE RING

We use the Luttinger model[20] in spherical approximation[21] to describe electronic states in the uppermost bulk valence band. In atomic units where $\hbar=m_0=1$, it reads

$$\mathcal{H}_s=\left(\frac{\gamma_1}{2}+\frac{\gamma_s}{2}\left[\hat{J}_z^2-\frac{5}{4}\right]\right)\hat{k}_\perp^2-\frac{\gamma_s}{2}(\hat{k}_-^2\hat{J}_+^2+\hat{k}_+^2\hat{J}_-^2)+\left(\frac{\gamma_1}{2}-\gamma_s\left[\hat{J}_z^2-\frac{5}{4}\right]\right)\hat{k}_z^2-\sqrt{2}\gamma_s(\{\hat{k}_z,\hat{k}_-\}\{\hat{J}_z,\hat{J}_+\}+\{\hat{k}_z,\hat{k}_+\}\{\hat{J}_z,\hat{J}_-\}). \quad (1)$$

Here, m_0 denotes the vacuum electron mass, $\gamma_s=(3\gamma_3+2\gamma_2)/5$ in terms of Luttinger parameters,[20] $\hat{\mathbf{k}}$ and $\hat{\mathbf{J}}$ are vector operators of kinetic linear and spin-3/2 angular momentum, respectively, and we used the notations

$\hat{\mathbf{k}}_\perp=(\hat{k}_x,\hat{k}_y)$, $\hat{k}_\pm=\hat{k}_x\pm i\hat{k}_y$, and $\hat{J}_\pm=(\hat{J}_x\pm i\hat{J}_y)/\sqrt{2}$. The symbol $\{A,B\}$ stands for the anticommutator $(AB+BA)/2$. When a quantum-well confinement in the growth (z) direction is introduced, two-dimensional (2D) subbands are formed. Here, we will focus on the situation wherein only the lowest 2D quantum-well bound state matters. To be specific, we assume a symmetric hard-wall confinement with a 2D quantum-well width d and simply replace the operators $\hat{k}_z^2$ and $\hat{k}_z$ with their respective expectation values π^2/d^2 and 0.[22] By using polar coordinates for in-plane motion, we obtain $\mathcal{H}_s^{(2D)}=\mathcal{H}_{sb}+\mathcal{H}_\perp^{(2D)}$, where

$$\mathcal{H}_{sb}=\left(\frac{\gamma_1}{2}-\gamma_s\left[\hat{J}_z^2-\frac{5}{4}\right]\right)\left(\frac{\pi}{d}\right)^2 \tag{2a}$$

arises from the quantized motion along the z direction, and the in-plane motion of holes is governed by the part

$$\mathcal{H}_\perp^{(2D)}=\left(\frac{\gamma_1}{2}+\frac{\gamma_s}{2}\left[\hat{J}_z^2-\frac{5}{4}\right]\right)\left\{-\partial_r^2-\frac{\partial_r}{r}+\frac{\hat{L}_z^2}{r^2}\right\}-\frac{\gamma_s}{2}\left(\hat{J}_+^2\left[-iL_-\left\{\partial_r+\frac{\hat{L}_z}{r}\right\}\right]^2+\hat{J}_-^2\left[-iL_+\left\{\partial_r-\frac{\hat{L}_z}{r}\right\}\right]^2\right). \tag{2b}$$

$\hat{L}_z=-i\partial_\varphi$ is the in-plane orbital angular momentum, and $L_\pm=e^{\pm i\varphi}$. Hamiltonian (2b) commutes with $\hat{M}_z=\hat{L}_z+\hat{J}_z$; hence, its eigenstates can be labeled by those of $\hat{M}_z$. To enable further analytic progress, we eliminate the φ dependence in off-diagonal matrix elements by the transformation $\tilde{\mathcal{H}}=e^{i\hat{J}_z\varphi}\mathcal{H}e^{-i\hat{J}_z\varphi}$. Due to space limitations, the straightforwardly obtained expression for the transformed Hamiltonian is omitted here.

The quasi-one-dimensional in-plane ring confinement is modeled by the singular-oscillator potential[23]

$$V_\perp(r)=\frac{\omega^2}{2}\left(r-\frac{R^2}{r}\right)^2, \tag{3}$$

which was employed before to study mesoscopic *electron* rings.[24] In the following, the energy scale $E_0=\pi^2\gamma_1\hbar^2/(2m_0d^2)$ associated with the 2D quantum-well confinement will serve as our energy unit. We also introduce the parameter $\bar{\gamma}=\gamma_s/\gamma_1$, which measures the strength of the spin-orbit coupling in the valence band; the length scale $\ell_\omega=\sqrt{\sqrt{\gamma_1}\hbar/(m_0\omega)}$ associated with the ring confinement; $\lambda_R=(R/\ell_\omega)^2$ and $\lambda_d=(2d/[\pi\ell_\omega])^2$, which represent the ring radius and the quantum-well width, respectively, in units of the effective ring width; and the operators $\hat{\Gamma}=1+\bar{\gamma}[\hat{J}_z^2-(5/4)]$ and $\hat{\varrho}=r/(\ell_\omega\hat{\Gamma}^{1/4})$, which quantify the HH-LH splitting. With these conventions, the Hamiltonian of a mesoscopic hole ring is $H\equiv(\tilde{\mathcal{H}}_s^{(2D)}+V_\perp)/E_0=H_{qw}+H_{rg}$, where

$$H_{qw}=1-2\bar{\gamma}\left[\hat{J}_z^2-\frac{5}{4}\right] \tag{4a}$$

arises from the HH-LH splitting in the quantum-well bound state, and the in-plane motion is governed by

$$H_{rg}=\frac{\lambda_d}{4}\hat{\Gamma}^{1/2}\left(-\partial_{\hat{\varrho}}^2-\frac{\partial_{\hat{\varrho}}}{\hat{\varrho}}+\frac{\hat{\tilde{L}}_z^2}{\hat{\varrho}^2}+\left[\hat{\varrho}-\frac{\lambda_R\hat{\Gamma}^{-1/2}}{\hat{\varrho}}\right]^2\right)+\frac{\lambda_d}{4}\bar{\gamma}\left\{\left(\hat{J}_+\hat{\Gamma}^{-1/4}\left[\partial_{\hat{\varrho}}+\frac{\hat{\tilde{L}}_z}{\hat{\varrho}}\right]\right)^2+\left(\hat{J}_-\hat{\Gamma}^{-1/4}\left[\partial_{\hat{\varrho}}-\frac{\hat{\tilde{L}}_z}{\hat{\varrho}}\right]\right)^2\right\}. \tag{4b}$$

Equation (4b) suggests the wave-function ansatz

$$\psi_{n,m}(r,\varphi)=e^{im\varphi}\begin{pmatrix}a_{n,m}\psi_{n,m}^{(3/2)}(r)\\ b_{n,m}\psi_{n,m}^{(1/2)}(r)\\ c_{n,m}\psi_{n,m}^{(-1/2)}(r)\\ d_{n,m}\psi_{n,m}^{(-3/2)}(r)\end{pmatrix}, \tag{5a}$$

where the four spinor amplitudes are given by

$$\psi_{n,m}^{(j)}(r)=\frac{\mathcal{N}_{n,m}^{(j)}}{\ell_\omega[1+2(|j|-1)\bar{\gamma}]^{1/4}}e^{-\varrho_j^2/2}\varrho_j^{\alpha_m^{(j)}}L_n^{(\alpha_m^{(j)})}(\varrho_j^2). \tag{5b}$$

$L_n^{(\alpha)}(x)$ is an associated Laguerre polynomial; $\mathcal{N}_{n,m}^{(j)}=[2\Gamma(n+1)/\Gamma(n+\alpha_m^{(j)}+1)]^{1/2}$, where $\Gamma(x)$ denotes the Euler Gamma function; $\varrho_j=r/\{\ell_\omega[1+2(|j|-1)\bar{\gamma}]^{1/4}\}$; and $\alpha_m^{(j)}=\sqrt{\{[(m-j)^2+\lambda_R^2/(1+2(|j|-1)\bar{\gamma})]\}}$. m is the eigenvalue of $\hat{M}_z$ and n is the oscillator-level index. Ansatz (5a) and (5b) diagonalizes the first term of Hamiltonian (4b),

$$H_{rg}^{(1)}=\lambda_d\left(\left[n+\frac{1}{2}\right]\hat{\Gamma}^{1/2}+\frac{\sqrt{\hat{\Gamma}(m-\hat{J}_z)^2+\lambda_R^2}-\lambda_R}{2}\right). \tag{6}$$

However, the second term of H_{rg} in Eq. (4b) is off-diagonal in spin-3/2 space, coupling HH and LH amplitudes

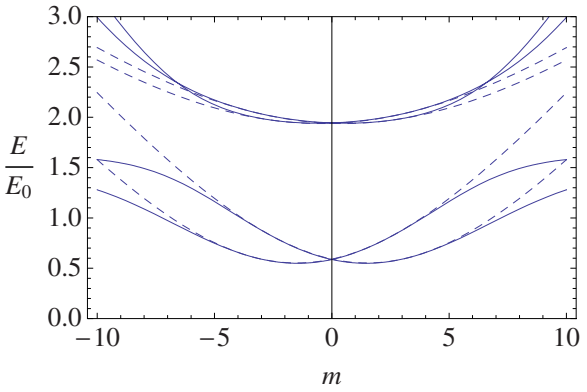

FIG. 1. (Color online) The lowest hole-ring subbands (solid curves) arising from the in-plane ring-potential bound-state level with $n=0$, calculated for $\bar{\gamma}=0.37$, $\lambda_d=0.5$, and $\lambda_R=10$. The dashed curves are obtained when HH-LH *splitting* is included but HH-LH *mixing* is neglected.

within subspaces spanned by $\hat{J}_z$ eigenstates with eigenvalues$\{\pm 3/2, \mp 1/2\}$, respectively. In addition, this term has both diagonal and off-diagonal matrix elements in the $\psi_{n,m}$ representation, i.e., it couples states with different n. We omit the lengthy analytical expressions for associated matrix elements. It turns out that the HH-LH mixing between states that have their quantum number n differ by 0, 1, and 2 are the most relevant. In the following, we focus on the lowest oscillator level ($n=0$) and include only its intralevel HH-LH mixing. Neglecting the subtle difference between ϱ_j and $\varrho_{j\pm 2}$, setting both equal to r/ℓ_ω, and replacing $\alpha_m^{(j)} \equiv \lambda_R$ yield the corresponding matrix element[25]

$$(H_{\rm rg}^{(2)})_{00} = -\frac{\lambda_d \bar{\gamma}}{4}\left\{\hat{J}_+^2\left[1-\frac{(m-\hat{J}_z-2)(m-\hat{J}_z)+2}{\lambda_R}\right] + \hat{J}_-^2\left[1-\frac{(m-\hat{J}_z+2)(m-\hat{J}_z)+2}{\lambda_R}\right]\right\}. \quad (7)$$

Diagonalizing the Hamiltonian $H_{\rm qw}+H_{\rm rg}^{(1)}+(H_{\rm rg}^{(2)})_{00}$ yields the lowest hole-ring subband dispersions. The result is shown in Fig. 1 for a set of realistic parameters. For comparison, we also plot the dispersions obtained when HH-LH *mixing* is neglected but HH-LH *splitting* is taken into account, i.e., when only $H_{\rm qw}+H_{\rm rg}^{(1)}$ is considered.

III. TWO-TERMINAL TRANSPORT AND AHARONOV-ANANDAN PHASE

At a fixed energy E between the HH-like and the LH-like subband bottoms shown in Fig. 1, four propagating channels exist, having different angular momenta $m_{s\sigma}$. Here, $s=+,-$ labels the two dispersion curves ($s=\pm$ corresponding to the subspace spanned by $\hat{J}_z$-projection eigenstates with eigenvalues $\{\pm 3/2, \mp 1/2\}$, respectively), and $\sigma=+,-$ distinguishes opposite propagation directions. The condition for finding these angular momenta is $E_s(m_{s\sigma})=E$. We now consider the following scenario, which is illustrated in Fig. 2. A lead attached at $\varphi=0$ is assumed to inject holes in a

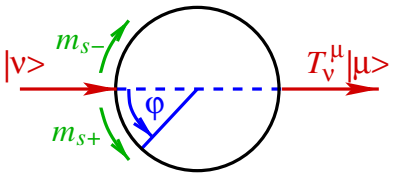

FIG. 2. (Color online) Two-terminal transport. The holes in scattering states $|\nu\rangle$ are injected via a lead attached at $\varphi=0$. Eigenmodes with angular momenta $m_{s\sigma}$ provide propagation channels in the ring. Upon reaching the point $\varphi=\pi$, interference and coupling into outgoing scattering states $|\mu\rangle$ occurs.

set of orthogonal initial states $|\nu\rangle$. Here, the ket refers to a normalized spin-3/2 spinor without any dependence on spatial coordinates.[26] Ring eigenstates taken at $\varphi=0$ and with spatial profile neglected are given by $\chi_{s\sigma}=(a_{0,m_{s\sigma}}, b_{0,m_{s\sigma}}, c_{0,m_{s\sigma}}, d_{0,m_{s\sigma}})$, and the injected states can be written as a superposition, namely, $|\text{in}\rangle_\nu=\Sigma_{s\sigma}\xi_{s\sigma}^{(\nu)}\chi_{s\sigma}$. Each spinor amplitude of a ring eigenstate with quantum numbers s,σ acquires a phase during propagation around a half-ring arm that is determined by its associated eigenvalue of the operator $\sigma\pi(\hat{M}_z-\hat{J}_z)$. The resulting state at $\varphi=\pi$ will be $|\text{out}\rangle_\nu=\Sigma_{s\sigma}\xi_{s\sigma}^{(\nu)}\chi_{s\sigma}\exp\{\sigma i\pi(m_{s\sigma}-\frac{3s}{2})\}$. Assuming another lead being attached at $\varphi=\pi$, we find the transmission probabilities from incoming-lead channel ν to outgoing-lead channel μ. When we include the effect of a finite magnetic flux ϕ threading the area bounded by the ring, it reads

$$T_\nu^\mu = \left|\sum_{s\sigma}\xi_{s\sigma}^{(\mu)*}\xi_{s\sigma}^{(\nu)}e^{\sigma i\pi\left(m_{s\sigma}+\frac{\phi}{\phi_0}-\frac{3s}{2}\right)}\right|^2. \quad (8)$$

In Eq. (8), $m_{s\sigma}\equiv -m_{-s,-\sigma}$ are the angular-momentum eigenvalues found for $\phi=0$. The linear two-terminal ring conductance is given by $G_{\rm rg}=\frac{e^2}{2\pi\hbar}\Sigma_{\nu,\mu}T_\nu^\mu$.

Inspection of Eq. (8) reveals the well-known signatures of the Aharonov-Bohm effect,[8] arising from the interference of counter-propagating modes with conserved quantum number s. A phase difference $\Phi_{\rm AA}^{(s)}$ of associated quantum amplitudes will be accumulated during propagation between $\varphi=0$ and π, which is essentially an Aharonov-Anandan phase[5] for holes confined in the ring. The latter can be written as the sum of a magnetic-flux–dependent part (the Aharonov-Bohm[2] phase $2\pi\phi/\phi_0$) and a remainder $\Phi_G^{(s)}$ that depends on the quantum number s distinguishing dispersion branches

$$\Phi_{\rm AA}^{(s)} = 2\pi\frac{\phi}{\phi_0}+\Phi_G^{(s)}, \quad (9a)$$

$$\Phi_G^{(s)} = \pi(m_{s+}+m_{s-}-3s). \quad (9b)$$

The symmetry $m_{s\sigma}=-m_{-s,-\sigma}$ which is fundamentally due to time-reversal invariance implies that $\Phi_G^{(+)}=-\Phi_G^{(-)}\equiv\Phi_G$. We plot Φ_G for a realistic set of parameters in Fig. 3.

IV. CONCLUSIONS AND DISCUSSION

We investigated the spin-3/2 hole states confined in a quasi-one-dimensional ring. A number of controlled approximations were employed that can be systematically improved

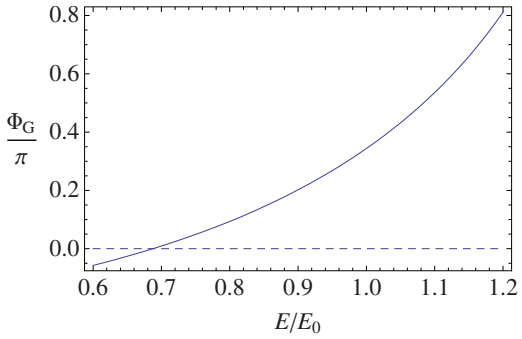

FIG. 3. (Color online) Solid curve: Anomalous component Φ_G of the AA phase appearing in the two-terminal hole-ring transmission. The parameters used in the calculation are the same as in Fig. 1. Dashed curve: Corresponding result obtained when HH-LH mixing is neglected.

upon. We find a previously neglected energy-dependent contribution Φ_G to the AA phase that results from HH-LH mixing and may be related to anomalous spin precession[27] of spin-3/2 particles. It is likely that this phase is the origin of numerically observed magneto-oscillations of the conductance polarization in multiply connected hole nanostructures[19] that persist even in the presence of relatively strong disorder. In a magnetoconductance experiment, the value $\Phi_G(E_F)$ of AA phase for states at the Fermi energy would be observed as a shift in the Aharonov-Bohm[2] oscillations. This mimics the behavior that is expected[12,13] in systems with a finite zero-field (Rashba or Dresselhaus) spin splitting that was used to interpret experimental data.[16] We show that, in general, both HH-LH mixing and spin-splitting effects need to be considered. In addition, the coupling of the ring to external leads needs to be well understood because the character of injected hole states will sensitively depend on the lead confinement.

ACKNOWLEDGMENTS

U.Z. thanks P. Brusheim and D. Csontos for useful discussions.

*Present address: Institut für Theoretische Physik A, RWTH Aachen, D-52056 Aachen, Germany.
†Permanent address: Institute of Fundamental Sciences and MacDiarmid Institute for Advanced Materials and Nanotechnology, Massey University, Private Bag 11 222, Palmerston North, New Zealand.

[1] *Geometric Phases in Physics*, edited by A. Shapere and F. Wilczek (World Scientific, Singapore, 1989).
[2] Y. Aharonov and D. Bohm, Phys. Rev. **115**, 485 (1959).
[3] Y. Aharonov and A. Casher, Phys. Rev. Lett. **53**, 319 (1984).
[4] M. V. Berry, Proc. R. Soc. London, Ser. A **392**, 45 (1984).
[5] Y. Aharonov and J. Anandan, Phys. Rev. Lett. **58**, 1593 (1987).
[6] J. Anandan, J. Christian, and K. Wanelik, Am. J. Phys. **65**, 180 (1997).
[7] *Mesoscopic Electron Transport*, edited by L. L. Sohn, L. P. Kouwenhoven, and G. Schön (Kluwer, Dordrecht, 1997).
[8] Y. Gefen, Y. Imry, and M. Y. Azbel, Phys. Rev. Lett. **52**, 129 (1984); M. Büttiker, Y. Imry, and M. Y. Azbel, Phys. Rev. A **30**, 1982 (1984).
[9] R. A. Webb, S. Washburn, C. P. Umbach, and R. B. Laibowitz, Phys. Rev. Lett. **54**, 2696 (1985); G. Timp, A. M. Chang, J. E. Cunningham, T. Y. Chang, P. Mankiewich, R. Behringer, and R. E. Howard, *ibid.* **58**, 2814 (1987).
[10] A. Stern, Phys. Rev. Lett. **68**, 1022 (1992); D. Loss and P. M. Goldbart, Phys. Rev. B **45**, 13544 (1992); A. G. Aronov and Y. B. Lyanda-Geller, Phys. Rev. Lett. **70**, 343 (1993).
[11] H. Mathur and A. D. Stone, Phys. Rev. Lett. **68**, 2964 (1992); T.-Z. Qian and Z.-B. Su, *ibid.* **72**, 2311 (1994).
[12] J. Nitta, F. E. Meijer, and H. Takayanagi, Appl. Phys. Lett. **75**, 695 (1999); D. Frustaglia and K. Richter, Phys. Rev. B **69**, 235310 (2004); B. Molnar, F. M. Peeters, and P. Vasilopoulos, *ibid.* **69**, 155335 (2004).
[13] A. A. Kovalev, M. F. Borunda, T. Jungwirth, L. W. Molenkamp, and J. Sinova, Phys. Rev. B **76**, 125307 (2007).
[14] I. Zutić, J. Fabian, and S. Das Sarma, Rev. Mod. Phys. **76**, 323 (2004).
[15] T. Bergsten, T. Kobayashi, Y. Sekine, and J. Nitta, Phys. Rev. Lett. **97**, 196803 (2006).
[16] M. König, A. Tschetschetkin, E. M. Hankiewicz, J. Sinova, V. Hock, V. Daumer, M. Schäfer, C. R. Becker, H. Buhmann, and L. W. Molenkamp, Phys. Rev. Lett. **96**, 076804 (2006); B. Grbić, R. Leturcq, T. Ihn, K. Ensslin, D. Reuter, and A. D. Wieck, *ibid.* **99**, 176803 (2007); B. Habib, E. Tutuc, and M. Shayegan, Appl. Phys. Lett. **90**, 152104 (2007); N. Kang, E. Abe, Y. Hashimoto, Y. Iye, and S. Katsumoto, J. Phys. Soc. Jpn. **76**, 083704 (2007).
[17] R. Winkler, *Spin-Orbit Coupling Effects in Two-Dimensional Electron and Hole Systems* (Springer, Berlin, 2003).
[18] HH and LH states correspond to eigenstates of spin-3/2 projection $\perp$ ring with eigenvalues $\pm 3/2$ and $\mp 1/2$, respectively.
[19] J. Zhou, M. W. Wu, and M. Q. Weng, Phys. Lett. A **349**, 393 (2006).
[20] J. M. Luttinger, Phys. Rev. **102**, 1030 (1956).
[21] N. O. Lipari and A. Baldereschi, Phys. Rev. Lett. **25**, 1660 (1970).
[22] Setting $\hat{k}_z \to 0$ neglects a subtle renormalisation of the effective hole masses for in-plane motion. See, e.g., E. L. Ivchenko and G. E. Pikus, *Superlattices and Other Heterostructures* (Springer, Berlin, 1995).
[23] W. Tan and J. C. Inkson, Semicond. Sci. Technol. **11**, 1635 (1996).
[24] W. C. Tan and J. C. Inkson, Phys. Rev. B **60**, 5626 (1999); M. Pletyukhov and V. Gritsev, *ibid.* **70**, 165316 (2004).
[25] Our approximations amount to neglecting higher-order corrections in $\bar{\gamma}$ and assuming $\lambda_R \gg |m|$, which is the typical regime of interest. The condition $\lambda_d < 1$ (required for neglecting higher 2D quantum-well bound states) is usually satisfied.
[26] The detailed form of spinor components in real space will influence the coupling of leads to the ring. However, this is irrelevant for the AA phase, which is our current focus.
[27] D. Culcer, C. Lechner, and R. Winkler, Phys. Rev. Lett. **97**, 106601 (2006).